IEEE Access
Multidisciplinary | Rapid Review | Open Access Journal

Received August 26, 2019, accepted September 9, 2019, date of publication September 18, 2019,
date of current version September 30, 2019.

Digital Object Identifier 10.1109/ACCESS.2019.2942195

Multi-Attribute Data Recovery in Wireless Sensor Networks With Joint Sparsity and Low-Rank Constraints Based on Tensor Completion

JINGFEI HE[1], YATONG ZHOU[1], GUILING SUN[2], AND TIANYU GENG[2]
[1]Tianjin Key Laboratory of Electronic Materials and Devices, School of Electronics and Information Engineering, Hebei University of Technology, Tianjin 300401, China
[2]College of Electronic Information and Optical Engineering, Nankai University, Tianjin 300071, China

Corresponding author: Jingfei He (hejingfei@hebut.edu.cn)

This work was supported in part by the National Natural Science Foundation of China under Grant 61801164 and Grant 61771262, in part by the Natural Science Foundation of Tianjin City under Grant 18JCQNJC01700, in part by the Natural Science Foundation of Hebei Province under Grant F2019202387, and in part by the Foundation of Hebei Education Department under Grant QN2018092.

ABSTRACT In wireless sensor networks (WSNs), data recovery is an indispensable operation for data loss or energy constrained WSNs using sparse sampling. However, the recovery accuracy is not satisfying for WSNs with various sensor types due to the neglect of the correlation among multi-attribute data. In this paper, we propose a novel data recovery method with joint sparsity and low-rank constraints based on tensor completion for multi-attribute data in WSNs. The proposed method represents the high-dimensional data as low-rank tensors to effectively exploit the correlation that exists in the multi-attribute data. The utilization of the spatiotemporal sparsity in the signal is emphasized by sparsity constraints. Furthermore, an algorithm based on the alternating direction method of multipliers is developed to solve the resultant optimization problem efficiently. Experimental results demonstrate that the proposed method significantly outperforms existing solutions in terms of recovery accuracy in WSNs.

INDEX TERMS Wireless sensor networks, data recovery, low-rank tensors, sparsity constraints, tensor singular value decomposition.

I. INTRODUCTION

Wireless sensor networks (WSNs) have been widely used in numerous applications including military surveillance, environmental monitoring, and health care monitoring, in which a number of sensor nodes monitor physical phenomena and transmit the data to a base station or sink node for processing [1], [2]. Due to the hardware and wireless conditions, data loss is common in WSNs, especially in large scale WSNs. Besides, to further reduce the energy consumption in energy constrained WSNs, one straightforward way is using sparse sampling to reduce the number of measurement (i.e., the collected data) [3], [4]. Both data loss situation and utilization of sparse sampling method result in the recovery problem to estimate the missing data in WSNs. Therefore, as an indispensable and important operation, data recovery becomes one of the key research issues in WSNs.

The associate editor coordinating the review of this manuscript and approving it for publication was Xianfu Lei.

Recently, a number of methods have been proposed for data recovery in WSNs, and these methods can be roughly partitioned into two categories: 1) methods exploiting the sparsity of the data in networks under various transform domains (e.g., the Distributed compressed sensing (DCS) method [5] and [6]) based on compressed sensing (CS) theory [7], and 2) methods which exploit the spatiotemporal correlation in the form of low-rankness (e.g., Efficient Data Collection Approach (EDCA) [8] and [9]–[11]) based on matrix completion [12]. Furthermore, methods utilizing both the low-rank and temporal sparsity feature were proposed [13], [14], and two stage matrix completion algorithm was also proposed to recover missing and corrupted values in WSNs [15], [16]. These proposed methods have achieved impressive results in data recovery in WSNs. However, when deal with the recovery of multi-attribute data in WSNs with various types of sensors, these methods still reconstruct each single attribute separately without utilizing the inherent correlation between different attributes. In fact, many physical attributes in the monitored environment have

strong correlation [17], [18]. Specifically, the temperature information may be influenced by the illumination in certain environments, which result in an inherent correlation between these two attributes. The utilization of correlation in multiple attributes has also been proposed in [18], [19] to further improve the recovery accuracy. These methods either exploit the sparsity or enforce the low-rankness through matricization methodologies. Actually, this inherent correlation can be more straightforwardly exploited using a high-order tensor model [20]–[24], which takes advantages of the correlation of the multi-attribute data along multiple directions.

The high order tensors, as a generalization of matrices and vectors, represent multidimensional data more efficiently and powerfully. More recently, the related tensor decomposition and tensor completion become the research hotspots and have been applied to various applications, such as image inpainting, magnetic resonance imaging, and face recognition. These tensor based methods yield impressive performances in multi-dimensional signal processing. Besides, several methods based on tensor have also been proposed for the data recovery in WSNs [25]–[27]. The tensor completion methods [25], [26] use latent variables based on CANDECOMP/PARAFAC (CP) [21] model to recover the data in heterogeneous sensor networks. However, due to the special structure of tensor consisting of WSNs data, the tensor methods based on CP perform unsatisfying in the data recovery in WSNs. Method [27] was proposed to utilize the tensor Singular Value Decomposition (t-SVD) [23] model for data recovery in WSNs and achieved better performances compared to the matricization methodologies. As a new tensor decomposition method, t-SVD has a similar structure to singular value decomposition in matrix, and many extensions to t-SVD have been developed [28], [29]. In fact, the t-SVD model, albeit useful, is not effective enough to exploit some underlying correlation of the WSNs data for completion. The spatiotemporal sparsity constraints can be jointly utilized to further improve the recovery accuracy.

In this paper, we propose a novel data recovery method with joint sparsity and low-rank constraints based on tensor completion for multi-attribute data in WSNs. The main contributions of this paper are as following:

Firstly, the proposed method extends the low-rank matrix based approach by using low-rank tensors to further exploit the inherent correlation among multiple attributes, beyond utilizing just spatiotemporal correlation in one attribute. Considering the features of the data in networks, t-SVD model is selected to exploit the correlation that exists in multiple attributes.

Secondly, the inherent correlation among multi-attribute data in WSNs is revealed using tensor decomposition based on two real datasets collected from GreenOrbs [30] and Intel Berkeley Research lab [31].

Thirdly, to further improve the recovery accuracy, the utilization of the spatiotemporal sparsity in multi-attribute data is emphasized with sparsity constraints. For solving the formulation incorporating the low-rank tensor and sparsity constraints terms, a reconstruction algorithm is also developed based on the alternating direction method of multipliers (ADMM) [32].

The rest of this paper is organized as follows: Section II presents the basics of tensor and t-SVD model; Section III reveals the correlation among multi-attribute data and details the proposed method and the reconstruction method. Section IV shows the representative simulation results and analyses, which is followed by the discussion in Section V and conclusion of the paper in Section VI.

II. BASICS ON TENSOR AND T-SVD

A tensor is a multidimensional array. The order of a tensor is the number of dimensions, i.e., vectors are the first order tensors, and matrices are the second order tensors. For tensors of order three or higher, the Euler script letters (e.g., $\mathcal{A}$) are utilized to denote these higher order tensors in this paper. Fibers of tensors are the higher-order analogue of rows and columns of matrix, which are defined by fixing every index but one. Similarly, slices are defined by fixing all but two indices. As a result, for a third order tensor $\mathcal{A} \in \mathbb{R}^{n_1 \times n_2 \times n_3}$, its column, row, and tube fibers are denoted by $\mathcal{A}(:, j, k)$, $\mathcal{A}(i, :, k)$, and $\mathcal{A}(i, j, :)$, respectively, and its horizontal, lateral, and frontal slices are denoted by $\mathcal{A}(i, :, :)$, $\mathcal{A}(:, j, :)$, and $\mathcal{A}(:, :, k)$, respectively.

There are several common forms for tensor decomposition used in signal processing, such as CP decomposition [21], [33], [34], Tucker decomposition [22], [35], [36], tensor train decomposition [37]–[39], and t-SVD [29], [40], [41]. CP decomposes a tensor as a sum of rank-one tensors, which can be considered as a higher-order extension of the matrix singular value decomposition, and Tucker decomposition is a form of higher-order principal component analysis. Indeed, CP model can be viewed as a special case of the Tucker model [42]. For an Nth order tensor $\mathcal{P}$, the Tucker model can be expressed as

$$\mathcal{P} = \mathcal{C} \times {}_1G^{(1)} \times {}_2G^{(2)} \times \cdots \times {}_NG^{(N)}. \tag{1}$$

where $\mathcal{C}$ is the core tensor and $G^{(1)}$ to $G^{(N)}$ are the factor matrices. The operator $\times_n$ denotes the n-model product. Based on different tensor decomposition models, a number of tensor completion methods have been proposed and yield impressive performances in several applications such as video inpainting [43] and magnetic resonance imaging [35]. However, the tensor completion methods based on CP model perform unsatisfying in the data recovery in WSNs [25], [26]. Actually, considering the features of the data in WSNs, t-SVD [23] model can be selected to exploit the correlation among multiple attributes and achieve satisfying performances [27]. In this paper, the method based on t-SVD model with the sparsity constraints is proposed to further improve the recovery accuracy. The following are some definitions and relevant mathematical properties for t-SVD [23], [41] to support our method.

Let $\mathcal{A} \in \mathbb{R}^{n_1 \times n_2 \times n_3}$ and $\mathcal{B} \in \mathbb{R}^{n_2 \times n_4 \times n_3}$, the t-product of $\mathcal{A}$ with $\mathcal{B}$ is denoted by $\mathcal{C} = \mathcal{A} * \mathcal{B}$ with size

$n_1 \times n_4 \times n_3$. Along the tube fibers, we have $\mathcal{C}(i,j,:) = \sum_{k=1}^{n_2} \mathcal{A}(i,k,:) \star \mathcal{B}(k,j,:)$, where $\star$ denotes the circular convolution. The tensor transpose of a tensor $\mathcal{A} \in \mathbb{R}^{n_1 \times n_2 \times n_3}$ is denoted by $\mathcal{A}^T \in \mathbb{R}^{n_2 \times n_1 \times n_3}$, which transposing each of the frontal slices of $\mathcal{A}$ and then reversing the order of transposed frontal slices through n_3. The real-valued tensor $\mathcal{Q}$ is orthogonal if $\mathcal{Q}^T * \mathcal{Q} = \mathcal{Q} * \mathcal{Q}^T = \mathcal{I}$, where $\mathcal{I}$ is the identity tensor whose first frontal slice is the identity matrix and all others are zero.

Based on the above definitions, the definition of t-SVD is as following: Let $\mathcal{A}$ be an $n_1 \times n_2 \times n_3$ real-valued tensor. Then the t-SVD of $\mathcal{A}$ is shown as $\mathcal{A} = \mathcal{U} * \mathcal{S} * \mathcal{V}^T$, where $\mathcal{U} \in \mathbb{R}^{n_1 \times n_1 \times n_3}$, $\mathcal{V} \in \mathbb{R}^{n_2 \times n_2 \times n_3}$ are orthogonal tensors, and $\mathcal{S}$ is an $n_1 \times n_2 \times n_3$ f-diagonal tensor (each frontal slice is a diagonal matrix).

It is noteworthy that the t-product in t-SVD can be computed efficiently by taking the fast Fourier transform (FFT) along the tube fibers of tensors. Let $\tilde{\mathcal{A}} = \mathscr{F}_3\mathcal{A}$ denote performing FFT along the tube fibers of $\mathcal{A} \in \mathbb{R}^{n_1 \times n_2 \times n_3}$ hereafter. For $\mathcal{C} = \mathcal{A} * \mathcal{B}$, $\tilde{\mathcal{C}}(:,:,i) = \tilde{\mathcal{A}}(:,:,i)\tilde{\mathcal{B}}(:,:,i)$ for $i \in \{1, 2, \cdots, n_3\}$ can be calculated first, and then $\mathcal{C}$ is obtained by taking an inverse FFT along the tube fibers of $\tilde{\mathcal{C}}$ (i.e., $\mathcal{C} = \mathscr{F}_3^{-1}\tilde{\mathcal{C}}$). Note that $\mathscr{F}_3$ and $\mathscr{F}_3^{-1}$ are the operators representing the FFT and inverse FFT along the tube fibers, respectively. The detail decomposition procedure of t-SVD for a third order tensor is shown in Algorithm 1.

Algorithm 1 t-SVD for a Third Order Tensor

Input: $\mathcal{A} \in \mathbb{R}^{n_1 \times n_2 \times n_3}$
$\tilde{\mathcal{A}} \leftarrow fft(\mathcal{A}, [\,], 3)$
for $i = 1$ *to* n_3 **do**
  $[\mathbf{U}, \mathbf{S}, \mathbf{V}] = svd\left(\tilde{\mathcal{A}}(:,:,i)\right)$
  $\tilde{\mathcal{U}}(:,:,i) = \mathbf{U}$; $\tilde{\mathcal{S}}(:,:,i) = \mathbf{S}$; $\tilde{\mathcal{V}}(:,:,i) = \mathbf{V}$;
Output: $\mathcal{U} \leftarrow ifft(\tilde{\mathcal{U}}, [\,], 3)$; $\mathcal{S} \leftarrow ifft(\tilde{\mathcal{S}}, [\,], 3)$;
$\mathcal{V} \leftarrow ifft(\tilde{\mathcal{V}}, [\,], 3)$;

Tensor completion based on t-SVD model penalizes the tensor complexity with tensor-nuclear-norm (TNN) denoted by $\|\mathcal{A}\|_{TNN}$. Specifically, $\|\mathcal{A}\|_{TNN}$, defined as the sum of the singular values of all the frontal slices of $\tilde{\mathcal{A}}$, is a valid norm and is the tightest convex relaxation to ℓ_1 norm of the tensor multi-rank (a vector with the i_{th} element equal to the rank of the i_{th} frontal slice of $\tilde{\mathcal{A}}$).

III. THE PROPOSED METHOD

A. PROBLEM FORMULATION

A WSN consisting of n various sensor nodes and sensing m different attributes is considered. Let N_j denote the jth node and A_k denote the kth attribute. Assume the sensor nodes sense and transmit the data to the sink once every τ time. As a result, during $t = p \times \tau$ time, total $n \times m \times p$ readings should be gathered in the sink as the multi-attribute data. Here, p denotes the number of time slots in monitoring period. The multi-attribute data can be organized into a third order tensor $\mathcal{M} \in \mathbb{R}^{n \times m \times p}$, as illustrated in Fig. 1. Data in column fiber $\mathcal{M}(:,k,i)$ represent readings of attribute A_k from different nodes at the ith time slot, and data in tube fiber $\mathcal{M}(j,k,:)$ represent readings of attribute A_k from node N_j at different time slots. The row fiber $\mathcal{M}(j,:,i)$ consists of different attribute readings from the node N_j at the ith time slot, and the number of attributes is usually small in most WSNs application. Thus, the row fiber is obviously short compared to the column fiber representing different sensor nodes and the tube fiber representing different collection time slots. As a result, the tensors consisting of WSNs data show the "narrow" property. Specifically, the i_{th} frontal slice of $\mathcal{M}$ can be expressed as

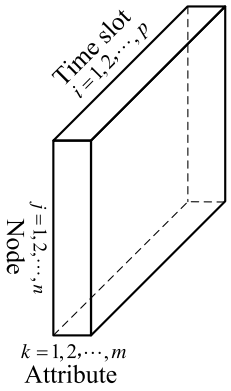

FIGURE 1. A third order tensor $\mathcal{M} \in \mathbb{R}^{n \times m \times p}$ consisting of multi-attribute data in WSNs.

$$\mathcal{M}^{(i)} = \begin{bmatrix} f(N_1, A_1, i) & \cdots & f(N_1, A_m, i) \\ \vdots & \ddots & \vdots \\ f(N_n, A_1, i) & \cdots & f(N_n, A_m, i) \end{bmatrix} \in \mathbb{R}^{n \times m}, \tag{2}$$

where $f\left(N_j, A_k, i\right)$ denotes the reading of attribute A_k from node N_j at time $t = i \times \tau$. It is worth noting that $f\left(N_j, A_k, i\right)$ corresponds to the element $\mathcal{M}(j,k,i)$ of the tensor.

However, in practice, there are only partial data can be transmitted to the sink due to data loss situation or sparse sampling method in WSNs. Let $\mathbf{d} \in \mathbb{R}^{D \times 1}$ denote the partially known data (i.e., the measurements) acquired from $\mathcal{M}$. Then we have $\mathbf{d} = \Omega(\mathcal{M})$, where $\Omega : \mathbb{R}^{n \times m \times p} \rightarrow \mathbb{R}^{D \times 1}$ is the operator to obtain the partially known data from the whole multi-attribute data. Therefore, the reconstruction method is of necessity for WSN to reconstruct the multi-attribute data $\mathcal{M}$ from the partial measurements $\mathbf{d}$ with size D ($D \ll nmp$). Here, we propose a novel method with sparsity constraints based on t-SVD to recover whole multi-attribute data from the partial measurement. Beyond just utilizing the spatiotemporal correlation in one attribute, the proposed method further exploits the inherent correlation among multiple attributes. Note that the time component is assigned to the tube direction to ensure a low tubal rank of $\mathcal{M}$, which is more suitable to the t-SVD model.

B. CORRELATION AMONG MULTI-ATTRIBUTE DATA

To verify the inherent correlation among multi-attribute data in WSNs with various types of sensors, two datasets gathered from GreenOrbs [30] and Intel Berkeley Research lab [31] were used as the sensor network testing data. Since data loss exists in both two datasets, two small but completed subset data are selected to obtain the ground truth, respectively. Specifically, the selected subset data of the GreenOrbs (denoted as GreenOrbs data hereafter) come from 130 sensors sensing three attributes for 129 time intervals, and the selected subset data of the Intel Berkeley Research lab (denoted as Berkeley data hereafter) come from 54 sensors sensing four attributes for 120 time intervals. The spatiotemporal correlation in one attribute can be verified by the low-rankness of the data matrix with singular value decomposition (SVD) [13]. In order to verify the correlation among multi-attribute data, the high order SVD (HOSVD) [44], [45], which is a generalization of the matrix SVD to tensor, can be adopted to the data tensor $\mathcal{M}$. The HOSVD computes a Tucker decomposition of the tensor and generates a core tensor $\mathcal{C}$ and corresponding factor matrices $\{\mathbf{G}^{(i)}\}_{i=1}^{3}$ via specifying the ranks.

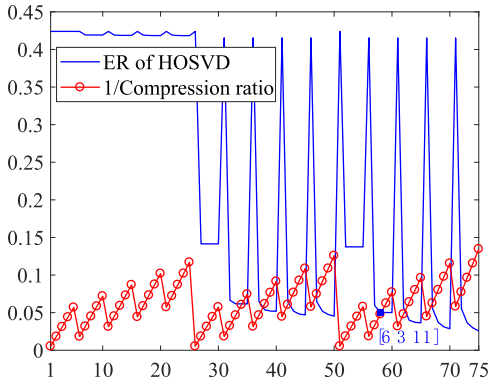

FIGURE 2. The ER of HOSVD of GreenOrbs data tensor with different Tucker ranks.

As shown in Fig. 2, the numerical values along x-axis denote the index of different Tucker ranks $\{[n_{1,i}, n_{2,j}, n_{3,k}]\}_{i=1,j=1,k=1}^{5,3,5}$, where $\{n_{1,i}\}_{i=1}^{5} = \{1, 6, 11, 16, 21\}$, $\{n_{2,j}\}_{j=1}^{5} = \{1, 2, 3\}$, $\{n_{3,k}\}_{k=1}^{5} = \{1, 6, 11, 16, 21\}$. Therefore, the number $(n_{1,i} + 25(n_{2,j} - 1) + (n_{3,k} - 1)/5)$ on x-axis indicates the Tucker rank $[n_{1,i}, n_{2,j}, n_{3,k}]$. The blue line indicates the error ratio (ER) of HOSVD of GreenOrbs data tensor, where ER is defined as

$$ER = \frac{\|\mathcal{C} \times_1 \mathbf{G}^{(1)} \times_2 \mathbf{G}^{(2)} \times_3 \mathbf{G}^{(3)} - \mathcal{M}\|}{\|\mathcal{M}\|}. \tag{3}$$

Here, the norm of a tensor is the square root of the sum of the squares of all its elements. The red line indicates the reduction in the degrees-of-freedom by $1/Compression\ ratio$, where Compression ratio is defined as

$$Compression\ ratio = \frac{n \times m \times p}{n_{1,i} \times n_{2,j} \times n_{3,k} + n_{1,i} \times n + n_{2,j} \times m + n_{3,k} \times p}. \tag{4}$$

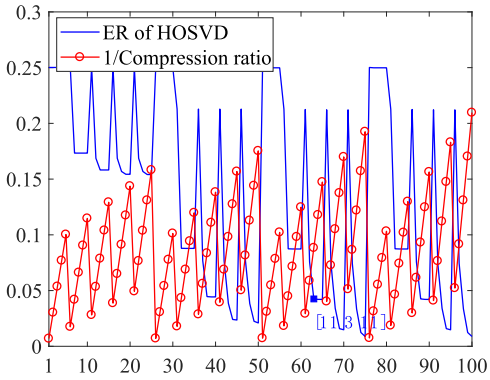

FIGURE 3. The ER of HOSVD of Berkeley data tensor with different Tucker ranks.

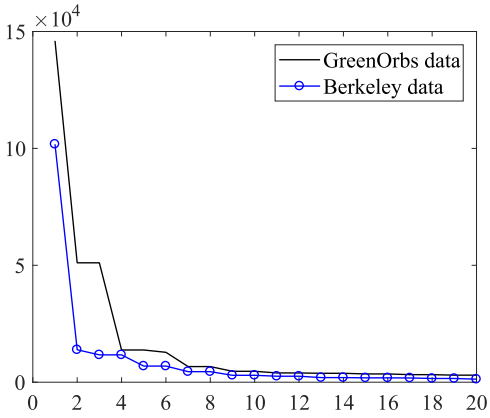

FIGURE 4. The first 20 singular values of the block diagonal matrix for GreenOrbs and Berkeley data.

Specifically, for Tucker rank specified as [6, 3, 11], the ER is less than 0.05 with Compression ratio larger than 20. Similar results can be obtained with the Berkeley data tensor, as shown in Fig. 3. The results indicate that the inherent correlation exists in multi-attribute data in WSNs, and the tensor methodologies can be utilized to exploit that correlation.

Although HOSVD method obtains satisfying results in verifying correlation among multi-attribute data, the HOSVD can not yield the best rank-r approximation in general. In this paper, the proposed method for multi-attribute data recovery in WSNs is mainly based on the t-SVD. In this subsection, the t-SVD is also utilized to verify the correlation among multi-attribute data. As shown in Fig. 4, the singular values of the block diagonal matrix illustrate the low-rankness for both two testing datasets. The block diagonal matrix [41] of $\tilde{\mathcal{M}}$ consists of all the frontal slices of the tensor $\tilde{\mathcal{M}}$ along the matrix diagonal. The rank of the block diagonal matrix is the tightest convex relaxation of the tensor-nuclear-norm of $\mathcal{M}$, which is mainly constrained in the t-SVD. Therefore, the correlation among multi-attribute data in WSNs can also be exploit by the t-SVD model.

C. TENSOR COMPLETION WITH JOINT SPARSITY AND LOW-RANK CONSTRAINTS

Let $\mathcal{X}$ represent the incomplete data tensor with $\Omega(\mathcal{X}) = \Omega(\mathcal{M})$, and the other entries in $\mathcal{X}$ are missing. Recovering

the missing entries of $\mathcal{X}$ is known as tensor completion, which has generated a great deal of research interest recently. According to the basics on t-SVD in Section II, the data in $\mathcal{X}$ can be recovered by solving the following formulation:

$$\begin{aligned} &\textit{minimize } \|\mathcal{X}\|_{TNN} \\ &\textit{subject to } \mathbf{d} = \Omega(\mathcal{X}). \end{aligned} \tag{5}$$

From the definition of the tensor-nuclear-norm, we have $\|\mathcal{X}\|_{TNN} = \sum_{i}^{p} \|\tilde{\mathcal{X}}^{(i)}\|_*$, where $\tilde{\mathcal{X}}^{(i)}$ is the i_{th} frontal slice of $\tilde{\mathcal{X}}$ and $\|\cdot\|_*$ the nuclear norm. Then (5) can be equivalently expressed as:

$$\begin{aligned} &\textit{minimize } \sum_{i}^{p} \left\|\tilde{\mathcal{X}}^{(i)}\right\|_* \\ &\textit{subject to } \mathbf{d} = \Omega\left(\mathscr{F}_3^{-1}\tilde{\mathcal{X}}\right). \end{aligned} \tag{6}$$

Here, $\mathscr{F}_3^{-1}\tilde{\mathcal{X}} = \mathcal{X}$ according to Section II. Besides, in order to improve the recovery accuracy, the utilization of the spatiotemporal sparsity is emphasized with sparsity constraints by the following formulation:

$$\begin{aligned} &\textit{minimize } \sum_{i}^{p} \left\|\tilde{\mathcal{X}}^{(i)}\right\|_* + \mu \left\|vec\left(\mathscr{F}_1\tilde{\mathcal{X}}\right)\right\|_1 \\ &\textit{subject to } \mathbf{d} = \Omega\left(\mathscr{F}_3^{-1}\tilde{\mathcal{X}}\right). \end{aligned} \tag{7}$$

where $vec(\mathscr{F}_1\tilde{\mathcal{X}})$ denotes the vector whose elements are taken columnwise from $\mathscr{F}_1\tilde{\mathcal{X}}$, μ the regularization parameter, and $\mathscr{F}_1$ is the operator representing the FFT along the column fibers. It is noteworthy that 2D Fourier transform of $\mathcal{X}$ is utilized for the spatiotemporal sparsity constraints in this paper. Essentially, each lateral slice of $\mathscr{F}_1\tilde{\mathcal{X}}$ is equal to performing 2D Fourier transform to each lateral slice of $\mathcal{X}$. The data in the kth lateral slice of $\mathcal{X}$ (i.e., $\mathcal{X}(:,k,:)$) contain readings of attribute A_k from different nodes at different time slots. Since these readings generated by the nodes in a certain area during a consecutive time are redundant and highly correlated, each lateral slice of $\mathcal{X}$ is sparse under the 2D Fourier transform. By enforcing the sparsity constraints $\left\|vec\left(\mathscr{F}_1\tilde{\mathcal{X}}\right)\right\|_1$, the utilization of the spatiotemporal sparsity in WSNs data is emphasized to further improve the recovery accuracy.

By introducing a quadratic penalty term, Eq. (7) can be converted as optimizing the following unconstrained formulation:

$$\begin{aligned} \hat{\tilde{\mathcal{X}}} &= \arg\min_{\tilde{\mathcal{X}}} \left\|\mathbf{d} - \Omega\left(\mathscr{F}_3^{-1}\tilde{\mathcal{X}}\right)\right\|_2^2 + \lambda \sum_{i}^{p} \left\|\tilde{\mathcal{X}}^{(i)}\right\|_* \\ &\quad + \mu \left\|vec\left(\mathscr{F}_1\tilde{\mathcal{X}}\right)\right\|_1 \\ \hat{\mathcal{X}} &= \mathscr{F}_3^{-1}\hat{\tilde{\mathcal{X}}} \end{aligned} \tag{8}$$

where λ and μ denote the regularization parameters. The regularization parameter λ and μ control the tunable tradeoff between the goal of achieving low-rankness of the tensor, presenting a spatiotemporal sparsity feature, and a precise fit to the data-fidelity term $\left\|\mathbf{d} - \Omega\left(\mathscr{F}_3^{-1}\tilde{\mathcal{X}}\right)\right\|_2^2$. The proposed method incorporates both the low-rank tensor constraints and sparsity constraints in a single formulation to further take advantage of the correlation of the multi-attribute data in WSNs. The solution to (8) reduces to the basic t-SVD method in (6) when $\mu = 0$. After $\hat{\tilde{\mathcal{X}}}$ is recovered in (8), the whole tensor $\hat{\mathcal{X}}$ can be generalized by taking an inverse FFT along the tube fibers of $\hat{\tilde{\mathcal{X}}}$, i.e., $\hat{\mathcal{X}} = \mathscr{F}_3^{-1}\hat{\tilde{\mathcal{X}}}$.

D. RECONSTRUCTION ALGORITHM BASED ON ADMM

Note that (8) is a convex optimization problem with nonsmooth regularization. Here, an efficient, globally convergent algorithm based on ADMM [32] is developed to solve it. The optimization equation in (8) can be converted into the following equivalent constrained optimization problem through variable splitting:

$$\begin{aligned} \{\hat{\tilde{\mathcal{X}}}, \mathcal{Z}, \mathcal{Y}\} = \arg\min_{\tilde{\mathcal{X}},\mathcal{Z},\mathcal{Y}} &\left\|\mathbf{d} - \Omega\left(\mathscr{F}_3^{-1}\tilde{\mathcal{X}}\right)\right\|_2^2 + \lambda \sum_{i}^{p} \left\|\mathcal{Z}^{(i)}\right\|_* \\ &+ \mu \|vec(\mathcal{Y})\|_1 \\ s.t.\ \mathcal{Z} = \tilde{\mathcal{X}}, &\quad \mathcal{Y} = \mathscr{F}_1\tilde{\mathcal{X}}. \end{aligned} \tag{9}$$

Then the augmented Lagrangian function for (9) can be written as

$$\begin{aligned} &\mathcal{L}(\tilde{\mathcal{X}}, \mathcal{Z}, \mathcal{Y}, \mathcal{A}, \mathcal{B}) \\ &= \left\|\mathbf{d} - \Omega\left(\mathscr{F}_3^{-1}\tilde{\mathcal{X}}\right)\right\|_2^2 \\ &\quad + \lambda \sum_{i}^{p} \left\|\mathcal{Z}^{(i)}\right\|_* + \left\langle \mathcal{A}, \mathcal{Z} - \tilde{\mathcal{X}} \right\rangle + \frac{\alpha}{2} \left\|\mathcal{Z} - \tilde{\mathcal{X}}\right\|_F^2 \\ &\quad + \mu \|vec(\mathcal{Y})\|_1 + \left\langle \mathcal{B}, \mathcal{Y} - \mathscr{F}_1\tilde{\mathcal{X}} \right\rangle + \frac{\beta}{2} \left\|\mathcal{Y} - \mathscr{F}_1\tilde{\mathcal{X}}\right\|_F^2, \end{aligned} \tag{10}$$

where $\mathcal{A}$ and $\mathcal{B}$ are two Lagrangian multipliers, and α and β are the penalty parameters related to convergence speed of the algorithm. Eq. (10) can be minimized by the following alternating direction method:

$$\tilde{\mathcal{X}}_{k+1} = \arg\min_{\tilde{\mathcal{X}}} \mathcal{L}(\tilde{\mathcal{X}}, \mathcal{Z}_k, \mathcal{Y}_k, \mathcal{A}_k, \mathcal{B}_k), \tag{11}$$

$$\mathcal{Z}_{k+1} = \arg\min_{\mathcal{Z}} \mathcal{L}(\tilde{\mathcal{X}}_{k+1}, \mathcal{Z}, \mathcal{A}_k), \tag{12}$$

$$\mathcal{Y}_{k+1} = \arg\min_{\mathcal{Y}} \mathcal{L}(\tilde{\mathcal{X}}_{k+1}, \mathcal{Y}, \mathcal{B}_k), \tag{13}$$

$$\mathcal{A}_{k+1} = \mathcal{A}_k + \alpha\left(\mathcal{Z}_{k+1} - \tilde{\mathcal{X}}_{k+1}\right), \tag{14}$$

$$\mathcal{B}_{k+1} = \mathcal{B}_k + \beta\left(\mathcal{Y}_{k+1} - \mathscr{F}_1\tilde{\mathcal{X}}_{k+1}\right). \tag{15}$$

The general solutions to the subproblems (11) to (13) and computational complexity analyses are described in Appendix. Specifically, the procedures of the reconstruction algorithm based on ADMM for solving (8) can be summarized in Algorithm 2.

Algorithm 2 The Reconstruction Algorithm for the Proposed Method

Input:
Initialized $\tilde{\mathcal{X}}_0$, $\mathcal{Z}_0$, $\mathcal{Y}_0$, $\mathcal{A}_0$, and $\mathcal{B}_0$;
The regularization parameters λ and μ and the penalty parameters α and β;
The measurements $\mathbf{d}$, the sampling operator Ω and the iteration number $k = 0$;
do
1) Iteration number $k = k + 1$;
2) Update $\tilde{\mathcal{X}}_k$ by solving (11);
3) Update $\mathcal{Z}_k$ by solving (12);
4) Update $\mathcal{Y}_k$ by solving (13);
5) Update $\mathcal{A}_k$ and $\mathcal{B}_k$ with(14) and (15);
while $\frac{\left\|\tilde{\mathcal{X}}_k - \tilde{\mathcal{X}}_{k-1}\right\|_F}{\left\|\tilde{\mathcal{X}}_{k-1}\right\|_F} \geqslant \epsilon$ ***and*** $k \leqslant K_{max}$;
Output: $\hat{\mathcal{X}} = \mathscr{F}_3^{-1}\tilde{\mathcal{X}}_k$;

In practical implementation, the $\tilde{\mathcal{X}}_0$, $\mathcal{Z}_0$, $\mathcal{Y}_0$, $\mathcal{A}_0$, and $\mathcal{B}_0$ are all initialized with zeros tensors. The algorithm is terminated when $\left\|\tilde{\mathcal{X}}_k - \tilde{\mathcal{X}}_{k-1}\right\|_F / \left\|\tilde{\mathcal{X}}_{k-1}\right\|_F$ is smaller than a predefined tolerance parameter ϵ, or k exceeds a maximum number of iterations K_{max}. It is worth noting that for the convex optimization problem in (8), the reconstruction algorithm based on ADMM is guaranteed to have global convergence from any initializations. With respect to the regularization parameters λ and μ, we can empirically choose them based on the prior information of the signal in the networks.

IV. EXPERIMENTS AND ANALYSIS

In order to evaluate the effectiveness of the proposed method for recovery of multi-attribute data in WSNs, the matricization methodologies including the sparsity constraint method [5] and the matrix completion method [8] and the tensor methodologies including the smooth PARAFAC tensor completion (SPC) [34], the low-rank tensor completion (LRTC) [43] and t-SVD [23], [27] are chosen for comparisons.

A. EXPERIMENTAL ENVIRONMENTS

The two subset data (i.e., the ground truth) adopted to verify the correlation among multi-attribute data are also utilized for the reconstruction experiments. The data loss or energy constrained WSNs using sparse sampling is considered in experiments. Therefore, only partial data (i.e., the measurements $\mathbf{d} \in \mathbb{R}^{D\times 1}$) can be gathered in the sink, while the other data are missing randomly due to data loss or unsampled in sparse sampling method. The missing ratio ρ is utilized to represent the ratio of the number of missing data to the number of whole data (i.e., the number of elements in $\mathcal{M}$).

Since we already have the ground truth from GreenOrbs and Intel Berkeley Research lab, the data missing procedure can be implemented by applying the random sampling operator Ω to the ground truth (i.e., data tensor $\mathcal{M} \in \mathbb{R}^{n\times m\times p}$, specifically, $\mathcal{M}_G \in \mathbb{R}^{130\times 3\times 129}$ for GreenOrbs data and $\mathcal{M}_B \in \mathbb{R}^{54\times 4\times 120}$ for Berkeley data) to obtain the measurements $\mathbf{d} = \Omega(\mathcal{M})$. In this case, the missing data are randomly distributed in the whole data tensor. The Error Ratio of Interest (*ERI*) was used to measure the recovery performances of different methods and defined as:

$$ERI = \frac{\sqrt{\sum_{i,j,k,(i,j,k)\in\Pi} |\mathcal{X}_{ijk} - \mathcal{M}_{ijk}|^2}}{\sqrt{\sum_{i,j,k,(i,j,k)\in\Pi} |\mathcal{M}_{ijk}|^2}}, \tag{16}$$

where Π represents the missing data subset of the complete set of entries $[n] \times [m] \times [p]$ (i.e., only errors on the missing data are counted in *ERI*).

In the simulation, the first step was to generate the sampling operator Ω to sample $\lfloor(1-\rho)nmp + \frac{1}{2}\rfloor$ entries in the whole data $\mathcal{M}$ and discard the other entries randomly. Then the measurements $\mathbf{d}$ can be calculated as the input for the reconstruction methods. The sparsity constraint method [5], the matrix completion method [8], SPC [34], LRTC [43], t-SVD [23], [27] and the proposed method were utilized to recover the whole data, respectively. After the reconstruction data were obtained, the corresponding *ERI* can be calculated. In our experiments, the process of randomly sampling and reconstruction were repeated 20 times for all the methods, and the average ERI results were presented. Besides, the regularization parameters of each method were manually selected to optimize their performances.

It should be noted since the matricization methodologies reconstruct each single attribute separately, $\lfloor(1-\rho)np + \frac{1}{2}\rfloor$ entries were random selected as the sampled data in each attribute for the sparsity constraint method and the matrix completion method. In order to compare these methods for each attribute, we selected the corresponding part of data to calculate the *ERI* (e.g., fixing $j = 1$ in (16) to compare the *ERI* of temperature information if $\mathcal{M}(:, 1, :)$ denotes the temperature data). For SPC method, the total variation (TV) was employed as a smoothness constraint to achieve better performances.

B. RECOVERY PERFORMANCE COMPARISONS

To compare the proposed method with the existing methods, four attributes in Berkeley data and three attributes in GreenOrbs data were utilized for the recovery performance comparisons. Fig. 5 to Fig. 8 show the recovery performance of each method for the four attributes: temperature, humidity, light, and voltage sensed in Intel Berkeley Research lab, respectively. Fig. 9 to Fig. 11 show the recovery performance of each method for the three attributes: temperature, humidity, and light sensed in GreenOrbs, respectively.

The numerical values on the x-axis denote the missing ratio ρ, while the numerical values on the y-axis represent *ERI*. To make the recovery performance comparisons more visible, the missing ratio was set from 0.8 to 0.99.

As can be seen, methods based on t-SVD obtain the lower *ERI* for almost every attributes in two testing datasets.

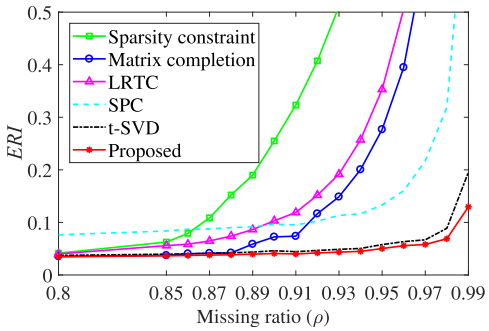

FIGURE 5. The recovery performance of each method for temperature data sensed in Intel Berkeley Research lab.

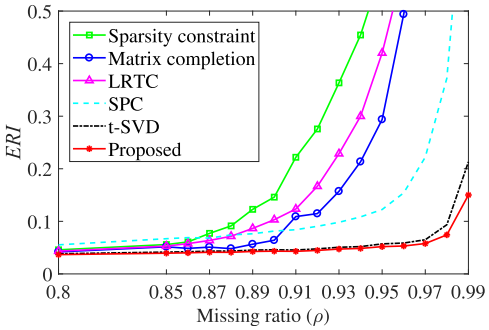

FIGURE 6. The recovery performance of each method for humidity data sensed in Intel Berkeley Research lab.

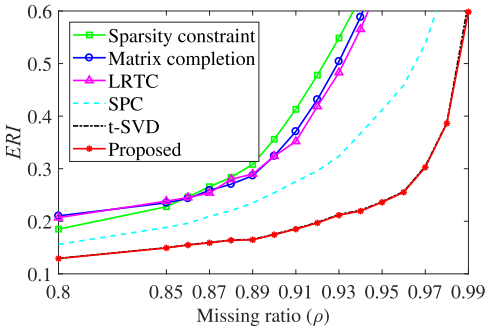

FIGURE 7. The recovery performance of each method for light data sensed in Intel Berkeley Research lab.

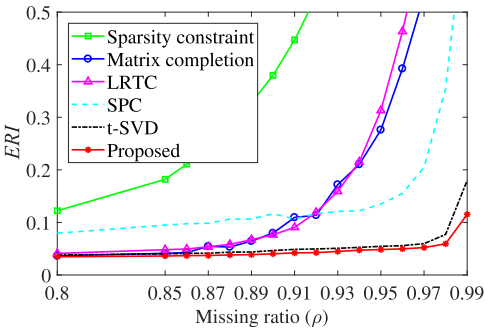

FIGURE 8. The recovery performance of each method for voltage data sensed in Intel Berkeley Research lab.

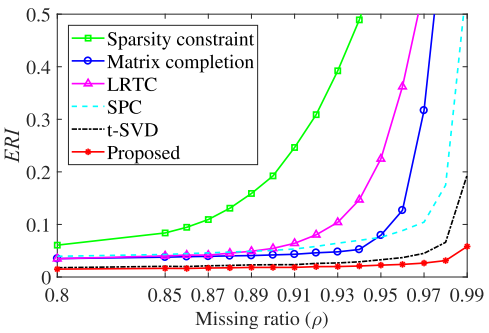

FIGURE 9. The recovery performance of each method for temperature data sensed in GreenOrbs.

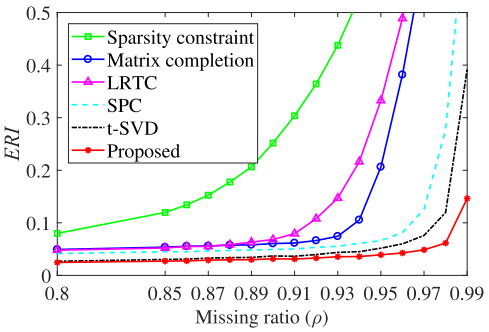

FIGURE 10. The recovery performance of each method for humidity data sensed in GreenOrbs.

And the proposed method performs better than the basic t-SVD method by emphasizing the spatiotemporal sparsity in multi-attribute data using sparsity constraints. Although the SPC and LRTC method are also based on the tensor model, they perform not well compared to the methods based on t-SVD. Actually, the LRTC method utilizes the low-rank constraints of the unfolded matrix along each mode. For the multi-attribute data in WSNs with the narrow property, the simulation results show that the low-rank completion method by tensor unfolding is not suitable.

As shown in Fig. 5, as the missing ratio increases to 0.9 or more, the corresponding recovery errors of sparsity constraint method, matrix completion method, SPC, and LRTC dramatically increase, while the *ERI* of the proposed method for temperature data is still below 0.1 even when the missing ratio is up to 0.98. Specifically, when the missing ratio is 0.99 (i.e., only 1% data are collected in the sink), the *ERI* of the proposed method and the basic t-SVD method are 0.130 and 0.196, respectively, while the *ERI* of the other methods are larger than 0.98. To ensure that the ERI of the reconstruction for Berkeley data is less than 0.05, the missing ratio for the proposed method should be lower than 94%, 94%, and 96% for temperature, humidity, and voltage data, respectively. The results show that the utilization of spatiotemporal sparsity in the proposed method can further improve the recovery accuracy, especially with large missing ratio.

The recovery errors for the light data sensed in Berkeley and GreenOrbs are shown in Fig. 7 and Fig. 11, respectively.

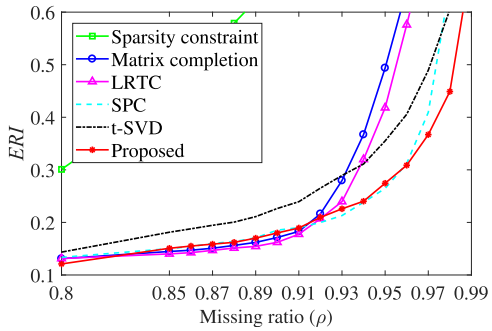

FIGURE 11. The recovery performance of each method for light data sensed in GreenOrbs.

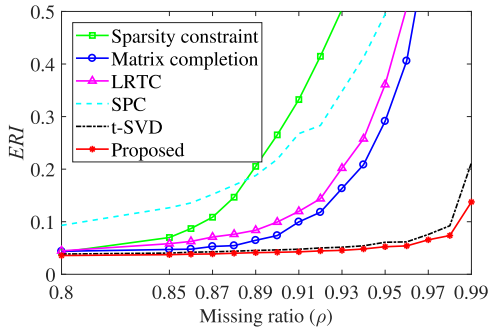

FIGURE 12. The recovery performance of each method for temperature data sensed in Intel Berkeley Research lab at SNR = 10dB.

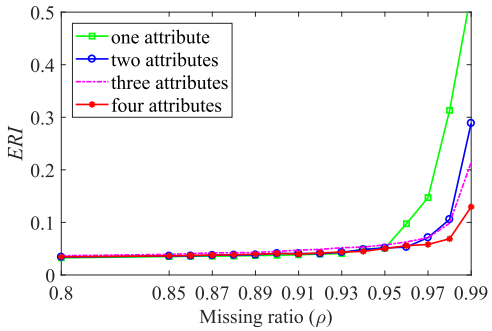

FIGURE 13. The recovery performance of the proposed method for temperature data sensed in Intel Berkeley Research lab with different number of attributes.

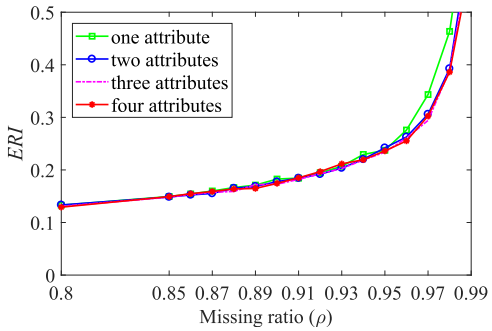

FIGURE 14. The recovery performance of the proposed method for light data sensed in Intel Berkeley Research lab with different number of attributes.

As can be seen, the above methods are all of poor performances, although the proposed method still performs better than the other methods. This is because the light data in both two testing datasets have looser spatiotemporal correlation. For the Berkeley light data, since the light data were collected from different rooms, the light data sensed by each sensor node were approximately independent. Although the light data were collected outdoors in GreenOrbs, the spatiotemporal correlation among the light data is weak for the existing of shade and the considerable variation of illumination in nature.

In order to demonstrate the efficiency of the proposed method, the situation in the presence of noise is also considered. In the simulation, the raw sensed data corrupted with noise were generated by adding the white Gaussian noise to each attribute with the specified signal-to-noise ratio (SNR). Fig. 12 shows the recovery performance of each method for temperature data sensed in Intel Berkeley Research lab at SNR = 10 dB. As can be seen, methods based on t-SVD exhibit the denoising effect in the presence of noise, and the proposed method results in the lowest ERI for different missing ratios. It demonstrates that the proposed method can achieve satisfying performance in both the absence and presence of noise.

C. RECOVERY PERFORMANCE WITH DIFFERENT NUMBER OF ATTRIBUTES

Consider the complex correlation among multiple physical attributes, tensor, as a multidimensional array, can represent the multi-attribute data more efficiently and have the potential of utilization of the complex correlation. Thus, we propose the recovery method with sparsity constraints based t-SVD to utilize the correlation among different attributes in WSNs. It raises a question that what is the relationship between the number of attributes and the data recovery accuracy.

In this subsection, in order to explore the influence of other attributes on the recovery of the selected attribute, the recovery performances with different number of attributes were compared. The recovery of temperature and light data sensed in Intel Berkeley Research lab were selected as the representatives for the experiment. Fig. 13 and Fig. 14 show the recovery performances of the proposed method for Berkeley temperature data and light data with different number of attributes, respectively.

Here, one attribute means only the selected attribute data (i.e., temperature data for Fig. 13 and light data for Fig. 14) are utilized in the proposed method for the data recovery in WSNs. The two attributes contain the selected attribute data and humidity data, and the three attributes contain temperature data, humidity data, and light data. The four attributes represent all the attributes sensed in the Berkeley data. As shown in Fig. 13, the proposed method utilizing more attributes obtains better recovery performance for the temperature data. Besides, the humidity data and the voltage data in Intel Berkeley Research lab with different number

of attributes have the similar recovery performances as the temperature data. However, Fig. 14 shows that for the Berkeley light data, the increase of the number of attributes has little influence on the recovery accuracy. Since the looser spatiotemporal correlation of the Berkeley light data, the recovery method can not take much advantage of the utilization of other attributes. It is interesting that although the other attributes can not improve the recovery accuracy of the light data, the light data can significantly improve the recovery of the other attributes.

V. DISCUSSION

The experimental results demonstrate that the proposed method yields significantly better performance than the compared existing methods. Theoretically, compared to the matricization methodologies (e.g., the sparsity constraint method and the matrix completion method), the proposed method uses the tensor model to represent multi-attribute data and benefits from utilization of correlation among multi-attribute data. Besides, considering the narrow property of WSNs data tensor, the selection of t-SVD model can achieve higher recovery accuracy than the low-rank completion method by tensor unfolding (e.g., LRTC method). Furthermore, compared with the basic t-SVD method, the proposed method can benefit from utilizing the sparsity constraints to emphasize the utilization of spatiotemporal sparsity.

It is also worth noting that the proposed method requires the selection of the regularization parameters λ and μ. We set $\lambda = 10, \mu = 1$ for Berkeley data and $\lambda = 10, \mu = 5$ for GreenOrbs data in our simulation experiments. The regularization parameters were manually selected for optimal performances, which was only possible when we have the ground truth. For now, automatic selection of optimal regularization parameters is still an open problem. The selection of regularization parameters in practical applications should be considered. Actually, for a large range of λ and μ values, the proposed method would produce similar recovery accuracy. As a result, we can initialize parameters according to the prior information of the signal in the networks.

VI. CONCLUSION

In this paper, we propose a novel data recovery method with joint sparsity and low-rank constraints based on tensor completion to increase the recovery accuracy for multi-attribute data in WSNs. The inherent correlation among multi-attribute data is revealed with the low-rank tensors for the testing dataset from GreenOrbs and Intel Berkeley Research lab. Based on the features of multi-attribute data in WSNs, t-SVD model is selected to effectively exploit the correlation, and enforcing the sparsity constraints is also utilized to emphasize the exploitation of spatiotemporal sparsity. Furthermore, an efficient algorithm was presented to solve the optimization problem based on ADMM. Although the algorithm requires the choice of the regularization parameters λ and μ, we can easily make selection with the prior information of the signal in the networks. The experimental results show that the proposed method outperforms the sparsity constraint method, matrix completion method, SPC, LRTC, and method based on t-SVD for each type of signals.

APPENDIX
SOLUTIONS FOR THE SUBPROBLEMS OF (10)

The general solutions to the subproblems (11) to (13) are established here. Note that (11) can be rewritten as

$$\begin{aligned}
&\tilde{\mathcal{X}}_{k+1} \\
&= \arg\min_{\tilde{\mathcal{X}}} \left\| \mathbf{d} - \Omega\left(\mathscr{F}_3^{-1}\tilde{\mathcal{X}}\right)\right\|_2^2 + \left\langle \mathcal{A}_k, \mathcal{Z}_k - \tilde{\mathcal{X}}\right\rangle \\
&\quad + \frac{\alpha}{2}\left\|\mathcal{Z}_k - \tilde{\mathcal{X}}\right\|_F^2 + \left\langle \mathcal{B}_k, \mathcal{Y}_k - \mathscr{F}_1\tilde{\mathcal{X}}\right\rangle + \frac{\beta}{2}\left\|\mathcal{Y}_k - \mathscr{F}_1\tilde{\mathcal{X}}\right\|_F^2 \\
&= \arg\min_{\tilde{\mathcal{X}}} \left\| \mathbf{d} - \Gamma(\tilde{\mathcal{X}})\right\|_2^2 + \frac{\alpha}{2}\left\|\mathcal{Z}_k - \tilde{\mathcal{X}} + \frac{\mathcal{A}_k}{\alpha}\right\|_F^2 \\
&\quad + \frac{\beta}{2}\left\|\mathcal{Y}_k - \Upsilon(\tilde{\mathcal{X}}) + \frac{\mathcal{B}_k}{\beta}\right\|_F^2
\end{aligned} \tag{A.1}$$

where $\Gamma(\tilde{\mathcal{X}}) = \Omega\left(\mathscr{F}_3^{-1}\tilde{\mathcal{X}}\right)$ and $\Upsilon(\tilde{\mathcal{X}}) = \mathscr{F}_1\tilde{\mathcal{X}}$ are linear operators. Note that (A.1) is a large-scale quadratic optimization problem, and the optimal solution to (A.1) is given by the following normal equations:

$$\begin{aligned}
&\left(\Gamma^*\Gamma + \frac{\alpha}{2} + \frac{\beta}{2}\Upsilon^*\Upsilon\right)\tilde{\mathcal{X}}_{k+1} \\
&\qquad = \Gamma^*(\mathbf{d}) + \frac{\alpha}{2}(\mathcal{Z}_k + \frac{\mathcal{A}_k}{\alpha}) + \frac{\beta}{2}\Upsilon^*(\mathcal{Y}_k + \frac{\mathcal{B}_k}{\beta}).
\end{aligned} \tag{A.2}$$

Here Γ^* and Υ^* are the Hermitian adjoint of the operator Γ and Υ, respectively. Since the operator $\Upsilon(\cdot)$ performs FFT along the column fibers of tensor, the operator $\Upsilon^*(\cdot)$ is equivalent to performing the inverse FFT along the column fibers. Thus we have

$$\begin{aligned}
\left(\Gamma^*\Gamma + \frac{\alpha+\beta}{2}\right)\tilde{\mathcal{X}}_{k+1} = \Big(&\Gamma^*(\mathbf{d}) + \frac{\alpha}{2}(\mathcal{Z}_k + \frac{\mathcal{A}_k}{\alpha}) \\
&+ \frac{\beta}{2}\Upsilon^*(\mathcal{Y}_k + \frac{\mathcal{B}_k}{\beta})\Big).
\end{aligned} \tag{A.3}$$

Eq. (A.3) can be efficiently solved by a number of numerical algorithms. Here, the preconditioned conjugate gradient (PCG) algorithm is applied in this paper, initialized with $\tilde{\mathcal{X}}_k$ to improve computational speed. The main computational cost to update $\tilde{\mathcal{X}}_{k+1}$ lies in the FFT operator. As a result, the computational complexity to update $\tilde{\mathcal{X}}_{k+1}$ in each iteration is $O\big(nmp\,(\log(n) + \log(p))\big)$.

Similarly, the subproblem (13) can be rewritten as

$$\begin{aligned}
\mathcal{Y}_{k+1} &= \arg\min_{\mathcal{Y}} \mu\|vec\,(\mathcal{Y})\|_1 + \left\langle \mathcal{B}_k, \mathcal{Y} - \mathscr{F}_1\tilde{\mathcal{X}}_{k+1}\right\rangle \\
&\quad + \frac{\beta}{2}\left\|\mathcal{Y} - \mathscr{F}_1\tilde{\mathcal{X}}_{k+1}\right\|_F^2 \\
&= \arg\min_{\mathcal{Y}} \mu\|vec\,(\mathcal{Y})\|_1 + \frac{\beta}{2}\left\|\mathcal{Y} - \mathscr{F}_1\tilde{\mathcal{X}}_{k+1} + \frac{\mathcal{B}_k}{\beta}\right\|_F^2.
\end{aligned} \tag{A.4}$$

Then the well-known soft-thresholding formula [46] can be utilized:

$$\mathcal{Y}_{k+1} = \mathcal{S}(\mathscr{F}_1\tilde{\mathcal{X}}_{k+1} - \frac{\mathcal{B}_k}{\beta}, \frac{\mu}{\beta}), \tag{A.5}$$

where $\mathcal{S}(\mathcal{Q}, \tau) : \mathbb{C}^{n\times m\times p} \to \mathbb{C}^{n\times m\times p}$ is a soft-thresholding operator defined as

$$\mathcal{S}(\mathcal{Q}, \tau)_{ijk} = \begin{cases} 0, & if \left|\mathcal{Q}_{ijk}\right| < \tau \\ \frac{\mathcal{Q}_{ijk}}{\left|\mathcal{Q}_{ijk}\right|}\left(\left|\mathcal{Q}_{ijk}\right| - \tau\right), & if \left|\mathcal{Q}_{ijk}\right| \geq \tau \end{cases} \tag{A.6}$$

for each element $\mathcal{Q}_{ijk}$ in $\mathcal{Q}$.

As for the subproblem (12), a similar procedure as above can be utilized. First, Eq. (12) can be simplified as:

$$\begin{aligned} \mathcal{Z}_{k+1} &= \arg\min_{\mathcal{Z}} \lambda \sum_{i}^{p} \left\|\mathcal{Z}^{(i)}\right\|_* + \left\langle \mathcal{A}_k, \mathcal{Z} - \tilde{\mathcal{X}}_{k+1}\right\rangle \\ &\quad + \frac{\alpha}{2}\left\|\mathcal{Z} - \tilde{\mathcal{X}}_{k+1}\right\|_F^2 \\ &= \arg\min_{\mathcal{Z}} \lambda \sum_{i}^{p} \left\|\mathcal{Z}^{(i)}\right\|_* + \frac{\alpha}{2}\left\|\mathcal{Z} - \tilde{\mathcal{X}}_{k+1} + \frac{\mathcal{A}_k}{\alpha}\right\|_F^2 \end{aligned} \tag{A.7}$$

The well-known singular value shrinkage formula [47] can be applied to solve (A.7). Furthermore, since exact SVD of the matrix with size $m \times n$ has time complexity $O(\min\{mn^2, m^2n\})$, in order to reduce the recovery time, the singular value shrinkage is utilized to each frontal slice of $\mathcal{Z}$ rather than the block diagonal matrix of $\mathcal{Z}$. For $\mathcal{Z} \in \mathbb{R}^{n\times m\times p}$, the time complexity reduces from $O(\min\{mn^2p^3, m^2np^3\})$ to $O(\min\{mn^2p, m^2np\})$. As a result, each frontal slice of $\mathcal{Z}$ is calculated in this paper. For the i_{th} frontal slice of $\mathcal{Z}$, we have

$$\mathcal{Z}_{k+1}^{(i)} = \arg\min_{\mathcal{Z}^{(i)}} \lambda\left\|\mathcal{Z}^{(i)}\right\|_* + \frac{\alpha}{2}\left\|\mathcal{Z}^{(i)} - \tilde{\mathcal{X}}_{k+1}^{(i)} + \frac{\mathcal{A}_k^{(i)}}{\alpha}\right\|_F^2. \tag{A.8}$$

Applying singular value shrinkage formula, we have

$$\mathcal{Z}_{k+1}^{(i)} = shrink(\tilde{\mathcal{X}}_{k+1}^{(i)} - \frac{\mathcal{A}_k^{(i)}}{\alpha}, \frac{\lambda}{\alpha}), \tag{A.9}$$

where $shrink(\mathbf{A}, \tau)$ is a nonlinear function which applies the soft-thresholding operator at level τ to the singular values of the matrix $\mathbf{A}$.

REFERENCES

[1] S. Kurt, H. U. Yildiz, M. Yigit, B. Tavli, and V. C. Gungor, "Packet size optimization in wireless sensor networks for smart grid applications," *IEEE Trans. Ind. Electron.*, vol. 64, no. 3, pp. 2392–2401, Mar. 2017.

[2] D. He, S. Zeadally, N. Kumar, and J.-H. Lee, "Anonymous authentication for wireless body area networks with provable security," *IEEE Syst. J.*, vol. 11, no. 4, pp. 2590–2601, Dec. 2017.

[3] X. Li, X. Tao, and G. Mao, "Unbalanced expander based compressive data gathering in clustered wireless sensor networks," *IEEE Access*, vol. 5, pp. 7553–7566, 2017.

[4] P. Sun, L. Wu, Z. Wang, M. Xiao, and Z. Wang, "Sparsest random sampling for cluster-based compressive data gathering in wireless sensor networks," *IEEE Access*, vol. 6, pp. 36383–36394, 2018.

[5] M. R. Duarte, M. B. Wakin, D. Baron, and R. G. Baraniuk, "Universal distributed sensing via random projections," in *Proc. 5th Int. Conf. Inf. Process. Sensor Netw. (IPSN)*, 2006, pp. 177–185.

[6] C. Lv, Q. Wang, W. Yan, and Y. Shen, "Diffusion wavelet basis algorithm for sparse representation of sensory data in WSNs," *Signal Process.*, vol. 140, pp. 12–31, Nov. 2017.

[7] D. L. Donoho, "Compressed sensing," *IEEE Trans. Inf. Theory*, vol. 52, no. 4, pp. 1289–1306, Apr. 2006.

[8] J. Cheng, H. Jiang, X. Ma, L. Liu, L. Qian, C. Tian, and W. Liu, "Efficient data collection with sampling in WSNs: Making use of matrix completion techniques," in *Proc. IEEE GLOBECOM*, Dec. 2010, pp. 1–5.

[9] L. Kong, M. Xia, X.-Y. Liu, G. Chen, Y. Gu, M.-Y. Wu, and X. Liu, "Data loss and reconstruction in wireless sensor networks," *IEEE Trans. Parallel Distrib. Syst.*, vol. 25, no. 11, pp. 2818–2828, Nov. 2014.

[10] K. Xie, X. Ning, X. Wang, D. Xie, J. Cao, G. Xie, and J. Wen, "Recover corrupted data in sensor networks: A matrix completion solution," *IEEE Trans. Mobile Comput.*, vol. 16, no. 5, pp. 1434–1448, May 2017.

[11] K. Xie, L. Wang, X. Wang, G. Xie, and J. Wen, "Low cost and high accuracy data gathering in WSNs with matrix completion," *IEEE Trans. Mobile Comput.*, vol. 17, no. 7, pp. 1595–1608, Jul. 2018.

[12] E. J. Candès and B. Recht, "Exact matrix completion via convex optimization," *Found. Comput. Math.*, vol. 9, no. 6, pp. 717–772, 2009.

[13] J. He, G. Sun, Y. Zhang, and Z. Wang, "Data recovery in wireless sensor networks with joint matrix completion and sparsity constraints," *IEEE Commun. Lett.*, vol. 19, no. 12, pp. 2230–2233, Dec. 2015.

[14] J. He, G. Sun, Z. Li, and Y. Zhang, "Compressive data gathering with low-rank constraints for wireless sensor networks," *Signal Process.*, vol. 131, pp. 73–76, Feb. 2017.

[15] N. Jain, A. Gupta, and V. A. Bohara, "PCI-MDR: Missing data recovery in wireless sensor networks using partial canonical identity matrix," *IEEE Wireless Commun. Lett.*, vol. 8, no. 3, pp. 673–676, Jun. 2019.

[16] N. Jain, A. Gupta, and V. A. Bohara, "TS-MC: Two stage matrix completion algorithm for wireless sensor networks," in *Proc. IEEE Int. Conf. Acoust., Speech Signal Process. (ICASSP)*, May 2019, pp. 7590–7594.

[17] M. G. Lawrence, "The relationship between relative humidity and the dewpoint temperature in moist air: A simple conversion and applications," *Bull. Amer. Meteorolog. Soc.*, vol. 86, no. 2, pp. 225–233, 2005.

[18] G. Chen, X.-Y. Liu, L. Kong, J.-L. Lu, Y. Gu, W. Shu, and M.-Y. Wu, "Multiple attributes-based data recovery in wireless sensor networks," in *Proc. Global Commun. Conf. (GLOBECOM)*, Dec. 2013, pp. 103–108.

[19] G. Chen, X.-Y. Liu, L. Kong, J.-L. Lu, and M.-Y. Wu, "Multi-attribute compressive data gathering," in *Proc. IEEE Wireless Commun. Netw. Conf. (WCNC)*, Apr. 2014, pp. 2178–2183.

[20] T. G. Kolda and B. W. Bader, "Tensor decompositions and applications," *SIAM Rev.*, vol. 51, no. 3, pp. 455–500, 2009.

[21] J. D. Carroll and J.-J. Chang, "Analysis of individual differences in multidimensional scaling via an n-way generalization of 'Eckart-Young' decomposition," *Psychometrika*, vol. 35, no. 3, pp. 283–319, Sep. 1970.

[22] L. R. Tucker, "Some mathematical notes on three-mode factor analysis," *Psychometrika*, vol. 31, no. 3, pp. 279–311, 1966.

[23] M. E. Kilmer, K. Braman, N. Hao, and R. C. Hoover, "Third-order tensors as operators on matrices: A theoretical and computational framework with applications in imaging," *SIAM J. Matrix Anal. Appl.*, vol. 34, no. 1, pp. 148–172, 2013.

[24] Z. Long, Y. Liu, L. Chen, and C. Zhu, "Low rank tensor completion for multiway visual data," *Signal Process.*, vol. 155, pp. 301–316, Feb. 2019.

[25] B. Milosevic, J. Yang, N. Verma, S. S. Tilak, P. Zappi, E. Farella, L. Benini, and T. S. Rosing, "Efficient energy management and data recovery in sensor networks using latent variables based tensor factorization," in *Proc. 16th ACM Int. Conf. Modeling, Anal. Simulation Wireless Mobile Syst. (MSWIM)*, 2013, pp. 247–254.

[26] B. Milosevic, C. Caione, E. Farella, D. Brunelli, and L. Benini, "Sub-sampling framework comparison for low-power data gathering: A comparative analysis," *Sensors*, vol. 15, no. 3, pp. 5058–5080, 2015.

[27] J. He, G. Sun, Y. Zhang, and T. Geng, "Data recovery in heterogeneous wireless sensor networks based on low-rank tensors," in *Proc. IEEE Symp. Comput. Commun. (ISCC)*, Jun. 2016, pp. 616–620.

[28] W. Hu, D. Tao, W. Zhang, Y. Xie, and Y. Yang, "The twist tensor nuclear norm for video completion," *IEEE Trans. Neural Netw. Learn. Syst.*, vol. 28, no. 12, pp. 2961–2973, Dec. 2016.

[29] Y. Liu, L. Chen, and C. Zhu, "Improved robust tensor principal component analysis via low-rank core matrix," *IEEE J. Sel. Topics Signal Process.*, vol. 12, no. 6, pp. 1378–1389, Dec. 2018.

[30] W. Dong, Y. Liu, Y. He, T. Zhu, and C. Chen, "Measurement and analysis on the packet delivery performance in a large-scale sensor network," *IEEE/ACM Trans. Netw.*, vol. 22, no. 6, pp. 1952–1963, Dec. 2014.
[31] *Sensor Data From Intel Berkeley Research Lab*. [Online]. Available: http://db.csail.mit.edu/labdata/labdata.html
[32] N. Parikh and S. Boyd, "Proximal algorithms," *Found. Trends Optim.*, vol. 1, no. 3, pp. 127–239, Jan. 2014.
[33] Y. Yang, Y. Feng, and J. A. K. Suykens, "A rank-one tensor updating algorithm for tensor completion," *IEEE Signal Process. Lett.*, vol. 22, no. 10, pp. 1633–1637, Oct. 2015.
[34] T. Yokota, Q. Zhao, and A. Cichocki, "Smooth PARAFAC decomposition for tensor completion," *IEEE Trans. Signal Process.*, vol. 64, no. 20, pp. 5423–5436, Oct. 2016.
[35] J. He, Q. Liu, A. G. Christodoulou, C. Ma, F. Lam, and Z.-P. Liang, "Accelerated high-dimensional MR imaging with sparse sampling using low-rank tensors," *IEEE Trans. Med. Imag.*, vol. 35, no. 9, pp. 2119–2129, Sep. 2016.
[36] Y. Liu, Z. Long, H. Huang, and C. Zhu, "Low CP rank and tucker rank tensor completion for estimating missing components in image data," *IEEE Trans. Circuits Syst. Video Technol.*, to be published.
[37] I. V. Oseledets, "Tensor-train decomposition," *SIAM J. Sci. Comput.*, vol. 33, no. 5, pp. 2295–2317, Jan. 2011.
[38] J. A. Bengua, H. N. Phien, H. D. Tuan, and M. N. Do, "Efficient tensor completion for color image and video recovery: Low-rank tensor train," *IEEE Trans. Image Process.*, vol. 26, no. 5, pp. 2466–2479, May 2017.
[39] Y. Liu, Z. Long, and C. Zhu, "Image completion using low tensor tree rank and total variation minimization," *IEEE Trans. Multimedia*, vol. 21, no. 2, pp. 338–350, Feb. 2019.
[40] M. E. Kilmer and C. D. Martin, "Factorization strategies for third-order tensors," *Linear Algebra Appl.*, vol. 435, no. 3, pp. 641–658, 2011.
[41] Z. Zhang and S. Aeron, "Exact tensor completion using t-SVD," 2015, *arXiv:1502.04689*. [Online]. Available: https://arxiv.org/abs/1502.04689
[42] N. D. Sidiropoulos, L. De Lathauwer, X. Fu, K. Huang, E. E. Papalexakis, and C. Faloutsos, "Tensor decomposition for signal processing and machine learning," *IEEE Trans. Signal Process.*, vol. 65, no. 13, pp. 3551–3582, Jul. 2017.
[43] J. Liu, P. Musialski, P. Wonka, and J. Ye, "Tensor completion for estimating missing values in visual data," *IEEE Trans. Pattern Anal. Mach. Intell.*, vol. 35, no. 1, pp. 208–220, Jan. 2013.
[44] L. De Lathauwer, B. De Moor, and J. Vandewalle, "A multilinear singular value decomposition," *SIAM J. Matrix Anal. Appl.*, vol. 21, no. 4, pp. 1253–1278, 2000.
[45] B. W. Bader and T. G. Kolda. *MATLAB Tensor Toolbox Version 2.5*. Accessed: Jan. 7, 2012. [Online]. Available: https://www.tensortoolbox.org
[46] D. L. Donoho, "De-noising by soft-thresholding," *IEEE Trans. Inf. Theory*, vol. 41, no. 3, pp. 613–627, May 1995.
[47] J.-F. Cai, E. J. Candes, and Z. Shen, "A singular value thresholding algorithm for matrix completion," *SIAM J. Optim.*, vol. 20, no. 4, pp. 1956–1982, 2010.

JINGFEI HE received the B.S. degree in electronic information science and technology and the Ph.D. degree in electronics science and technology from Nankai University, China, in 2012 and 2017, respectively.

From 2014 to 2015, he was a Visiting Scholar with the Department of Electrical and Computer Engineering, University of Illinois at Urbana-Champaign, USA. He is currently an Assistant Professor with the Hebei University of Technology. His research interests include wireless sensor networks, magnetic resonance imaging, and high-dimensional signal processing.

YATONG ZHOU received the B.E. and M.E. degrees in applied geophysics from the Chengdu University of Technology, China, in 1995 and 1999, respectively, and the Ph.D. degree in information and communication engineering from Xi'an Jiaotong University, China, in 2006.

He worked previously with the Bureau of Geophysical Prospecting (BGP), CNPC, and the Institute of Geology and Geophysics, Chinese Academy of Sciences, as a Postdoctoral Fellow. He has visiting experiences at Peking University, Wake Forest University, and The University of Texas at Austin. He is currently a Professor with the Hebei University of Technology. His research mainly focuses on machine learning, intelligent information processing, and seismic signal processing.

GUILING SUN received the Ph.D. degree from Nankai University, China, in 2004.

She is currently a Professor with the College of Electronic Information and Optical Engineering, Nankai University. She is also the Vice Director of the Tianjin Institute of Communications, the Vice Director of EDA Technology Research Society in North China, the Leader of Electronic Technology Experiment, and a Practice Teaching Team of Tianjin city. Her research interests include the wireless sensor networks, compressed sensing, information detection, and signal processing.

TIANYU GENG received the B.S. degree in electronics science and technology from Nankai University, China, in 2014, where he is currently pursuing the Ph.D. degree in electronics science and technology.

From 2018 to 2019, he was a Visiting Scholar with the Department of Electrical Engineering, Columbia University, USA. His research interests include wireless sensor networks, compressed sensing, and image processing.